Characterization of the Superstition Hills fault, Southern California, ruptured in the 1987 M6.6 earthquake, using fault-zone trapped waves

Award #00HQGR0030

Yong-Gang Li
Department of Earth Sciences
University of Southern California,
Los Angeles, CA 90089-0740.
Tel: 213-740-3556
Fax: 213-740-8801
E-mail: ygli@terra.usc.edu

Collaborators:
Michael J. Rymer
U.S. Geological Survey
(605)-329-5649
mrymer@usgs.gov

Rufus D. Catchings
U.S. Geological Survey
(650)-329-4749
catching@usgs.gov

Key words: Fault-Zone Trapped Waves, Fault Zone Structure, and Earthquake Physics

Non-technical Summary

We carried out a seismic experiment at the Superstition Hills fault to characterize the internal structure and segmentation of the rupture zone of the 1987 *M*6.6 earthquake. Observations and numerical modeling of fault-zone trapped waves generated by near-surface explosions and microearthquakes and recorded at seismic arrays deployed across and along the rupture zone show that the rupture zone is marked by a low-velocity zone ~75 m wide where the shear velocities are reduced by 25-30% from wall-rock velocities. Fault-zone trapped waves infer that the northwest and southeast rupture segments connected at the seismogenic depth and overlapped at least 4 km in the step-over. The SHF may dip to southwestward with the epicentral locations of most aftershocks on the southwest side of the fault trace at surface. The northern rupture segment is marked by a relatively simple low-velocity waveguide with the higher velocity reduction within the rupture zone than the southeast rupture segment that may abut to a blind fault (the northwest extension of the Wiener fault) on the southwest side.

The greater postseismic slips might attribute to the multiple subsurface fault strands lie on the southwest side of the surface fault trace.

We expect that a thorough analysis and modeling of the data recorded at the USGS Texan reflection lines across the overlapped part of the northwest and southeast rupture segments will provide additional details of the internal structure of the SHF around the step-over.

Non-technical Summary

We carried out a seismic experiment at the Superstition Hills fault to characterize the internal structure and segmentation of the rupture zone of the 1987 *M*6.6 earthquake. Observations and numerical modeling of fault-zone trapped waves generated by near-surface explosions and microearthquakes and recorded at seismic arrays deployed across and along the rupture zone show that the rupture zone is marked by a low-velocity zone ~75 m wide where the shear velocities are reduced by 25-30% from wall-rock velocities. Fault-zone trapped waves infer that the northwest and southeast rupture segments connected at the seismogenic depth and overlapped at least 4 km in the step-over. The SHF may dip to southwestward with the epicentral locations of most aftershocks on the southwest side of the fault trace at surface. The northern rupture segment is marked by a relatively simple low-velocity waveguide with the higher velocity reduction within the rupture zone than the southeast rupture segment that may abut to a blind fault (the northwest extension of the Wiener fault) on the southwest side.

Reports published

A manuscript on characterization of the rupture zone of the 1987 *M*6.6 Superstition Hills, California earthquake from fault-zone trapped waves is in preparation by Li, Rymer and Rufus.

Data Availability

The data recorded at 50 REFTEKs for explosions and microearthquakes are available from the P.I. Yong-Gang Li at USC. The Texan data are available from collaborators of this project, Rufus Catchings and Michael Rymer of USGS, Menlo Park.

References

Frankel, A. and L. Wennerberg (1989). Rupture process of the M6.6 Superstition Hills, California, earthquake determined from strong-motion recordings: Application of tommographic source inversion, Bull. Seismo. Soc. Am., 79, 515-541.

Magistrale H., L. Jones, and H. Kanamori (1989). The Superstition Hills, California, earthquakes of 24 November 1987, Bull. Seismo. Soc. Am., 79, 239-251.

McGill, S. F., C. R. Allen, K. W. Hudnut, D. C. Johnson, W. F. Miller, and K. E. Sieh (1989). Slip on the Superstition Hills fault and on nearby faults associated with the 24 November 1987 Elmore Ranch and Superstition Hills earthquakes, southern California, Bull. Seismo. Soc. Am., 79, 342-361.

Sharp R. V. K. E. Budding, J. Boatwright, M. J. Ader, M. G. Bonilla, M. M. Clark, T. E. Fumal, K. K. Harms, J. J. Lienkaemper, D. M. Morton, B. J. O'Neill, C. L. Ostergren, D. J. Ponti, M. J. Rymer, J. L. Saxton, and J. D. Sims, Surface faulting along the Superstition Hills fault zone and nearby faults associated with the earthquakes of 24 November 1987 (1989). Bull. Seismo. Soc. Am., 79, 252-281.

Characterization of the Superstition Hills fault, Southern California, ruptured in the 1987 *M*6.6 earthquake, using fault-zone trapped waves

Award #00HQGR0030

Yong-Gang Li
Department of Earth Sciences
University of Southern California,
Los Angeles, CA 90089-0740.
Tel: 213-740-3556
Fax: 213-740-8801
E-mail: ygli@terra.usc.edu

Collaborators:
Michael J. Rymer
U.S. Geological Survey
(605)-329-5649
mrymer@usgs.gov

Rufus D. Catchings
U.S. Geological Survey
(650)-329-4749
catching@usgs.gov

Key words: Fault-Zone Trapped Waves, Fault Zone Structure, and Earthquake Physics

Introduction

The 1987 *M*6.6 Superstition Hills, southern California, earthquake occurred on the right-lateral Superstition Hills fault (SHF) zone which ruptured along 24 km of its entire length and a bit more along Wienert fault (WF) that was not mapped previously (Figure1). The SHF is composed by two major segments that is distinguished by a right stepping zone of complex faulting. The northern and southern segments are approximately 15 km and 12 km in the length, respectively. The two fault strands overlap about a 4 km-long zone. The southwestward termination of the north strand is complex. A fault mapped in the Pleistocene beds extends at least 1.3 km beyond and parallel to the southernmost set of continuous surface breaks. The combination of the older fault and the location of the continuous new rupture suggests that the past slip events there have had greater lengths and possibly larger displacements than the 1987 event [*Sharp et al.*, 1989]. On the other hand, the north end of the southern rupture segment overlaps the north strand about 4 km, with a stepover feature that lies only 60 to 270 m away from the opposing strand (Figure 2). A large number of north- or northeast-trending fractures formed between the overlapping strands. On the part of the south strand near Imler Road, displayed an exceptionally complex fracture pattern. Right-lateral movement occurred on many subsidiary fractures on both sides of the fault, defining a zone of rupture at least 350 m wide.

The displacement caused by the 1987 earthquake was continuing to grow with afterslip along nearly the entire length of the rupture. It is note that each fault segment displayed prolonged postseismic creep. Each of these faults lies in an area where crystalline basement rocks are covered by a thick sedimentary layer. The post-seismic slips along the entire rupture length on the SHF continued after the 1987 event, with the overall maximum final displacement about 112 mm on the southern strand (Figure 2b). There were two distinct minima in displacements; one at the right-stepovers between the northern and southern strands of the SHF, and another step-over between the SHF and WF. The greater postseismic dextral slip occurred near the fault than farther from the fault. Figure 2a shows that the movement decreased sharply at distances greater than ~150 m southwest of the south SHF strand near Imler Road [*McGill et al.*, 1989]. It is also note that most aftershocks of the *M*6.6 event occurred on the southwest side of the SHF [*Magistrale et al.*, 1989], suggesting the SHF probably dips southwestward at seismogenic depth.

The rupture process in the SHF earthquake is quite different from those determined for other earthquakes (e.g., 1966 Parkfield; 1979 Imperial Valley; 1984 Morgan Hill; 1992 Landers). The overall rupture process was slow in developing. The high-frequency subevents were confined to the north strand of the SHF. However, the south strand did not generate significant high-frequency strong ground motion, but showed substantial co-seismic surface displacement. The high frequency component on the north strand was probably determined by asperities while the lower stress drop on the south strand might produce the long-period seismic energy [*Frankel and Wennerberg*, 1989]. The strong-motion station PTS located 55 m from the SHF break nearby Imler Road exhibited larger horizontal acceleration with lower frequencies than those registered at other stations farther away from the fault [*Frankel and Wennerberg*, 1989], showing the trapping efficiency of the low-velocity fault-zone waveguide. The geological mapping, geodetic and seismological observations show that multiple fault segments with different characteristics were involved in the rupture of the 1987 earthquake.

In order to delineate the internal structure and physical properties of the Superstition rupture zone with high resolution, we carried out an seismic using near-surface explosions detonated within the rupture zone. We deployed dense linear seismic arrays deployed across and along the rupture zone to record fault-zone trapped waves generated by explosions and microearthquakes. In this report, we exhibit fault-zone trapped waves recorded at the 1987 Superstition Hills rupture zone and used these waves to construct a structural model of the fault zone. The results will help further understand the relationship between the fault geometry and rupture process in earthquake.

Results from fault-zone trapped waves at the SHF

In November of 2000, we deployed two 500-m-long linear seismic arrays, each array consisting of 21 PASSCAL REFTEKs with three-component 2 Hz L22 sensors, across the Superstition Hills fault in the Navy Base near El Centro, southern California (Figure 1). The two arrays, called north Array 1 and south Array 2, were ~4 km apart from each other, and crossed the 1987 northern and southern rupture segments around the step-over between tow segments, respectively (Figure 2b). The north array was centered at the surface break of the northwest fault strand while the south array was centered at the surface break of the southeast fault strand. The southwest part of the north Array 1 also transected the northwest extension of the southeast fault

strand while the northeast part of the south Array 2 transected the southeast extension of the northwest fault strand in the step-over. The station spacing of the cross-fault array was 12.5 m for 9 stations in the middle part of the array, and 25 m and 50 m for farther stations. At each station, three components of the 2 Hz L22 sensor (Mark product) were in the vertical, and parallel and perpendicular to the fault trace. We also deployed a 1.4-km-long array of 8 REFTEKs with the station spacing 200-m along the southern rupture segment. The along-fault seismic line passed the cross-fault south Array 1 at the co-located station ST0 to form a cross-shape array. The REFTEK recorders worked in the event-trigger mode. The recording length was 90 s with the sample rate of 500 samples per second for explosions. The recording length was 40 s with the sample rate of 100 samples per second for microearthquakes.

The USGS seismic team led by Rufus Catchings and Michael Rymer (collaborators of this project) deployed 178 PASSCAL TEXANs with 4.5 and 40 Hz vertical-component geophones along two lines across the fault step-over between the southern and northern rupture segments (the middle array in Figure 1 and Figure 2a). Line 1 was 400 m long and included 108 geophones while line 2 was 170 m long and included 70 geophones.

We detonated 2 explosions SP1 and SP2 on November 18, using 550 and 350 pounds of chemical emulsions, respectively; in 80-feet-deep cased shot holes drilled within the southern and northern rupture segments, respectively. Shot SP1 was located ~4 km southeast of the south Array 2 while SP2 was located ~1 km northwest of the north Array 1 (Figure 1 and Figure 2b). The latitude and longitude are 32N55.5 and 115W41.8 at shot SP1, and 32N58.31 and 115W45.71 at shot SP2. The timing of seismic recorders and origin times of explosions were synchronized by the GPS. The USGS team made 80 gunshots along two lines at the middle array after recording explosions, and then retrieved all TEXAN instruments from the field.

After explosions, the south Array 1 and along-fault array remained in the field to record microearthquakes for 24 days between November 18 and December 12 while the northern array was retrieved from the field due to security consideration. The cross-shape array of 28 REFTEKs were triggered by ~200 events during this time period. ~120 events among them were micro- and remote earthquakes. 40 events were microearthquakes with *P*-to-*S* arrival time less then 3 s. These 40 microearthquakes occurred within a distance range of ~20 km from Array 2. Only 2 of them were located by the regional seismic network; one occurred on Nov. 26, ~15 km east and another occurred on Nov. 28, ~20 km northeast of Array 2. Other events are too small to trigger the regional network stations but they triggered our near-fault tight array. ~20 tiny earthquake recorded at our array showed good signal-to-noise ratio but only a few of them generated fault-zone trapped waves, suggesting that most tiny earthquakes occurred out of the fault zone.

So far we have completed waveform analysis of the data recorded at 50 REFTEKs deployed in 3 linear seismic lines across and along the Superstition Hills fault. We recorded fault-zone trapped waves generated by 2 bore-hole explosions detonated within the 1987 rupture zone and generated by microearthquakes occurring in the fault zone during our experiment in November, 2000. Since fault-zone trapped waves arise from constructive interference of multiple reflections at the boundaries between the low velocity fault zone and high velocity surrounding rocks, the amplitudes and dispersion of these waves are strongly dependent on the geometry and material

properties of the fault zone. Observations and 3-D finite-difference modeling of fault-zone trapped waves allowed us to insight into the internal structure and continuation of the Superstition Hills rupture zone.

Figures 3 to 6 show three-component seismograms in the across-fault and along-fault profiles recorded for explosions and microearthquake. Fault-zone trapped waves with relatively large amplitudes at 3-6 Hz and long duration are prominent at stations of arrays located close to the 1987 surface rupture on the north and south SHF strand in a distance range about 75 m from the fault trace. We used 3-D finite-difference code [*Graves,* 1996] to simulate Superstition Hill fault-zone trapped waves. Figure 7 shows example of synthetic trapped waves in terms of the structural model shown in Figure 8. The synthetics are comparable with observations in Figs. 3a and 4b in the zero-order sense. The model parameters will be refined furthermore using all recorded data. In summary,

(1) Fault-zone trapped waves show the existence of low-velocity waveguides along the northwest and southeast rupture segments of the 1987 Superstition Hills earthquake. The low-velocity waveguides are ~75 m wide where shear velocities are reduced by 25-30% from wall-rock velocities and Q values of 10-80 between the surface and seismogenic depth (Figure 8).

(2) We interpret that the low-velocity waveguides on the SHF are the remnant of the dynamic rupture in the 1987 M6.6 mainshock. The width of process zone (damage zone) delineated by trapped waves scales to the rupture length as some existing rupture model predicted [e.g. *Scholz,* 1990].

(3) Trapped waves indicate that the two rupture segments connect at depth beneath step-over at surface (Figure 8b). The array located on one rupture segment (e.g. Array 1 on the northwest fault strand) registered fault-zone trapped waves generated by the shot on the opposite rupture segment (e.g. the southeast shot SP1 on the south fault strand).

(4) We found that the low-velocity waveguides either on the northwest or on the southeast rupture segments at depth overshot in the length longer than the surface breaks in the step-over because the cross-fault arrays recorded trapped waves at both fault strands (Figs. 3 to 6). The distance between Array 1 and Array 2 is 4 km, meaning that the overlapping part of two rupture segments at depth is at least 4 km in the length although the surface ruptures in the step-over are less than this length.

(5) The low-velocity waveguide on the northwest rupture segment lies at the southwest side of the surface fault trace (Fig. 3a), suggesting the fault dips to southwest, consistent with the distribution pattern of 1987 aftershocks shown in Fig. 1.

(6) The northwest rupture segment is marked by a simple low-velocity waveguide with higher velocity contrast between fault zone and wall rocks than the southeast rupture segment is (Fig. 8).

(7) Because the waves with large amplitudes and long duration also appeared at stations near the southwest end of Array 2 (Figs. 4 and 6), we speculate that there exists a blind fault parallel to the SHF south strand. It may be the northwest extension of the Wiener fault, which ruptured in the 1987 earthquake too. This blind fault may connect to the SHF at depth (Fig. 8b). Post-seismic displacement measurements showed larger slips on the southwest side of the southeast rupture segment in a distance range of ~150 m from the SHF south strand [*McGill ET al.*, 1989].

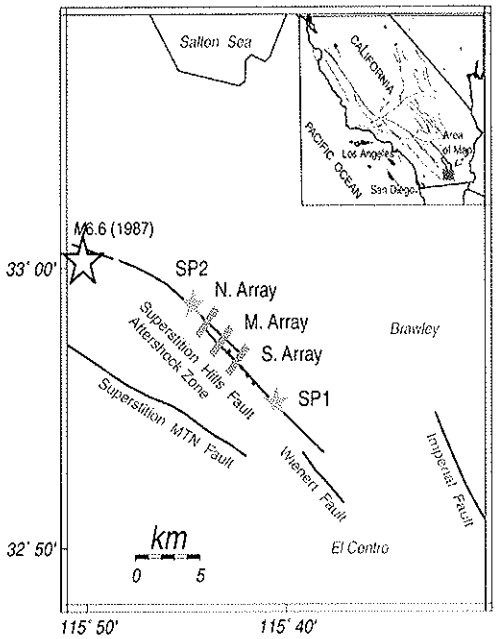

Figure 1. The locations of linear seismic arrays (grey bars labeled N. Array, S. Array and M. Array) deployed across the Superstition Hills fault, and explosions (stars labeled SP1 and SP2) detonated within the rupture zone of the 1987 M6.6 Superstition Hills, California, earthquake. Solid dots are stations deployed along the fault. Black lines show mapped active faults. The entire length of the Superstition Hills fault and Wienert fault ruptured and exposed to surface in the 1987 mainshock. The big star is the M6.6 mainshock on Nov. 24, 1987. The shaded zone denotes the epicentral area of 1987 M6.6 earthquake [Magistrale et al., 1989]. Most aftershocks occurred on the southwest side of the SHF. The inset shows the location of the area of map.

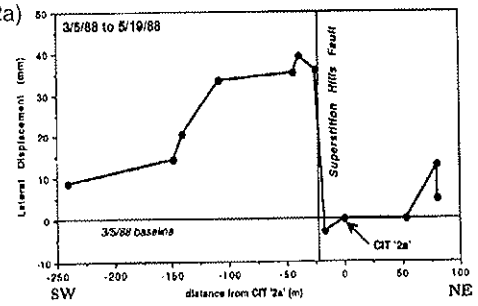

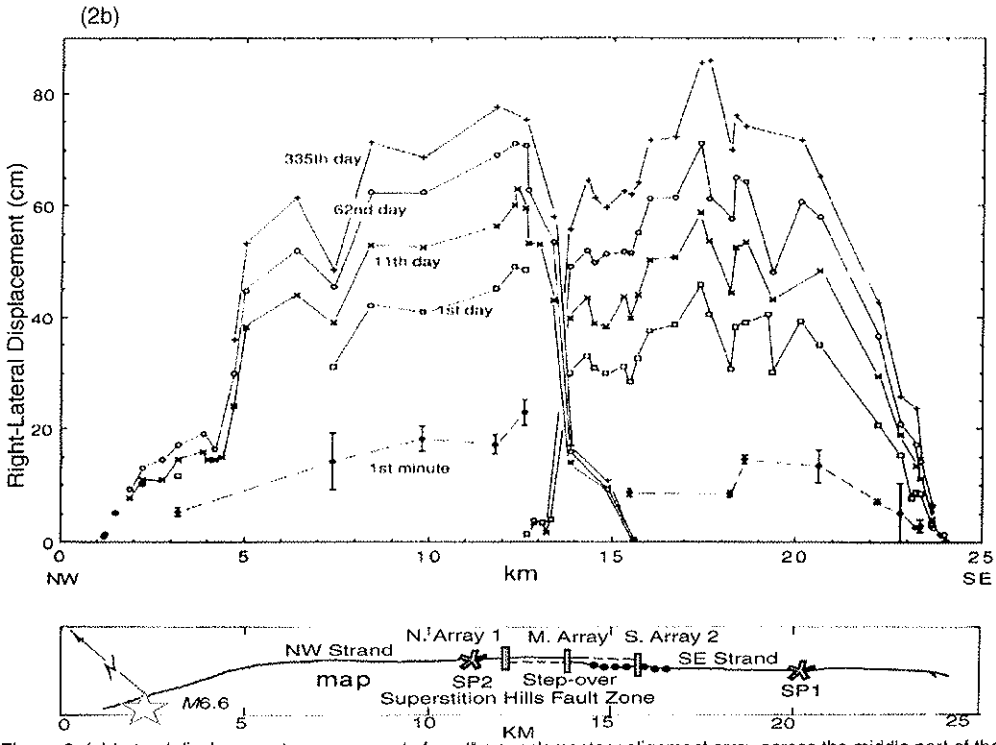

Figure 2. (a) Lateral displacement measurements from the supplementary alignment array across the middle part of the southeast fault strand of the Superstition Hills fault near Imler Road in the period March 5 to May 19, 1988 [McGill et al., 1989]. The data clearly show less right-lateral displacement with increasing distance greater than ~100 m from the fault trace. Note that the maximum postseismic displacement occurred at the southwest side of the fault. (b) top: Longitudinal profile of right-lateral component of slip along the SHF observed on November 25, December 5 and 6, 1987, and on January 25 and October 24, 1988 [Patrick and Magistrale, 1989]. bottom: The map view of the Superstition Hills fault zone. The fault zone is composite of the northwest and southeast strands with smaller displacements occurring in the step-over. The seismic arrays and explosions (grey bars and stars) are projected on the map. Solid dots are station along the fault. The black lines are new surface breaks in the 1987 M6.6 mainshock. The dashed lines denote the end parts of fault strands in the step-over, on which the surface breaks were unclear.

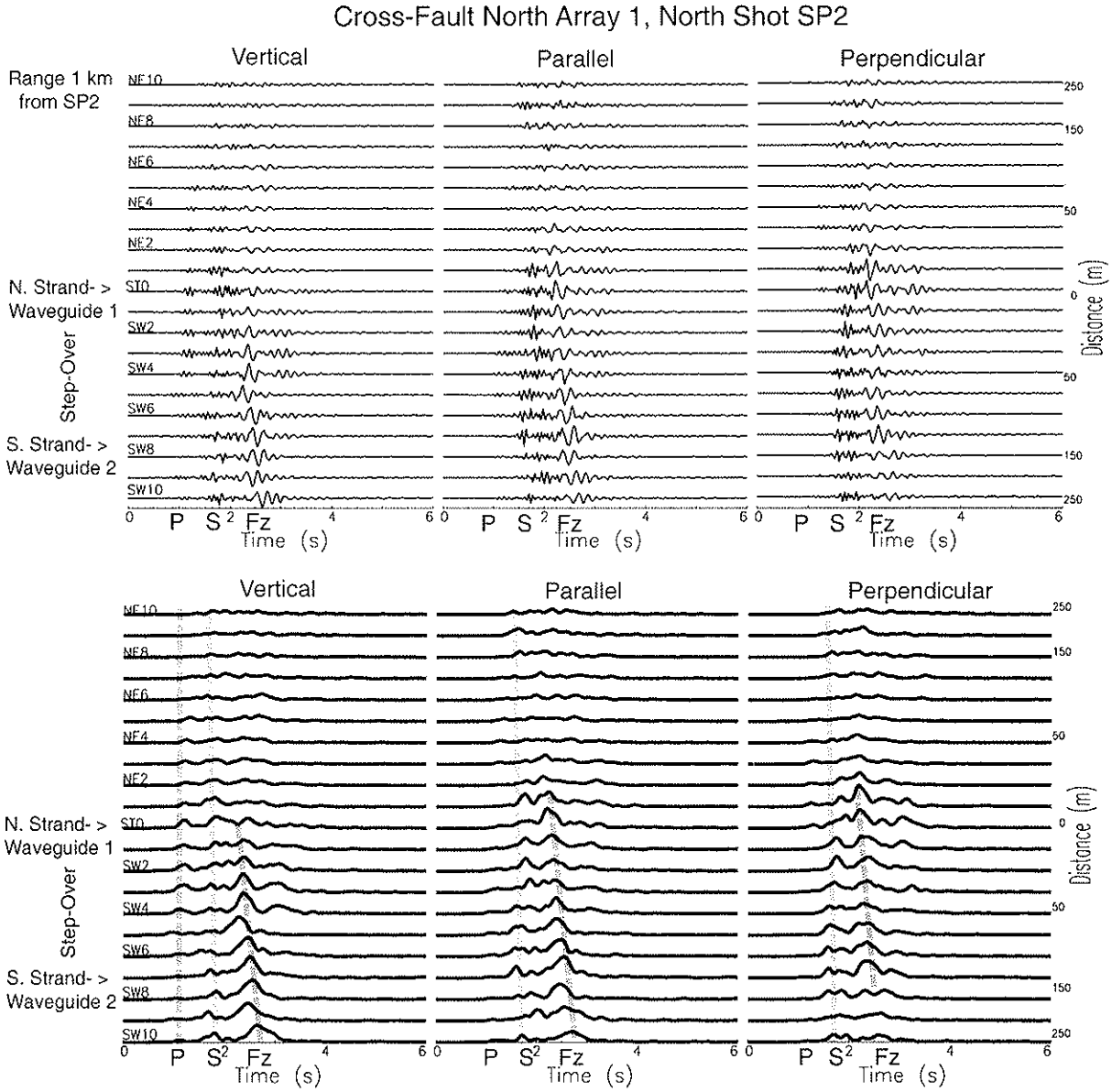

Figure 3a. top: Three-component seismograms recorded at the north Array 1 across the SHF in the step-over for the north shot SP2 detonated within the northwest rupture segment at the distance (range) of 1 km northwest of the array in November 18, 2000. The array was 500-m long with uneven station spacings, plotted at right of seismograms. Station names beginning with NE or SW denote the station located northeast or southwest of the fault trace. Station ST0 of the array was located on the northwest fault strand while the southwest part of the array intersected the extension of the southeast fault strand in the step-over. Seismograms have been low-pass (< 15 Hz) filtered and are plotted using a common scale for all traces. P and S waves arrive at ~0.8 s and ~1.5 s. Fault-zone trapped waves (Fz) with large amplitudes and long duration following S waves at stations on the southwest part of the array. bottom: Envelopes of waveforms are plotted using a common scale for all traces, showing large amplitudes of trapped waves at stations on the southwest part of the array that were located in the fractured damage zone in the step-over between the northwest and southeast rupture segments. The red, green, and blue dashed lines align with the peaks of P, S, and trapped waves, respectively. Note that the separation between S and trapped waves increases with distance between the shot and stations.

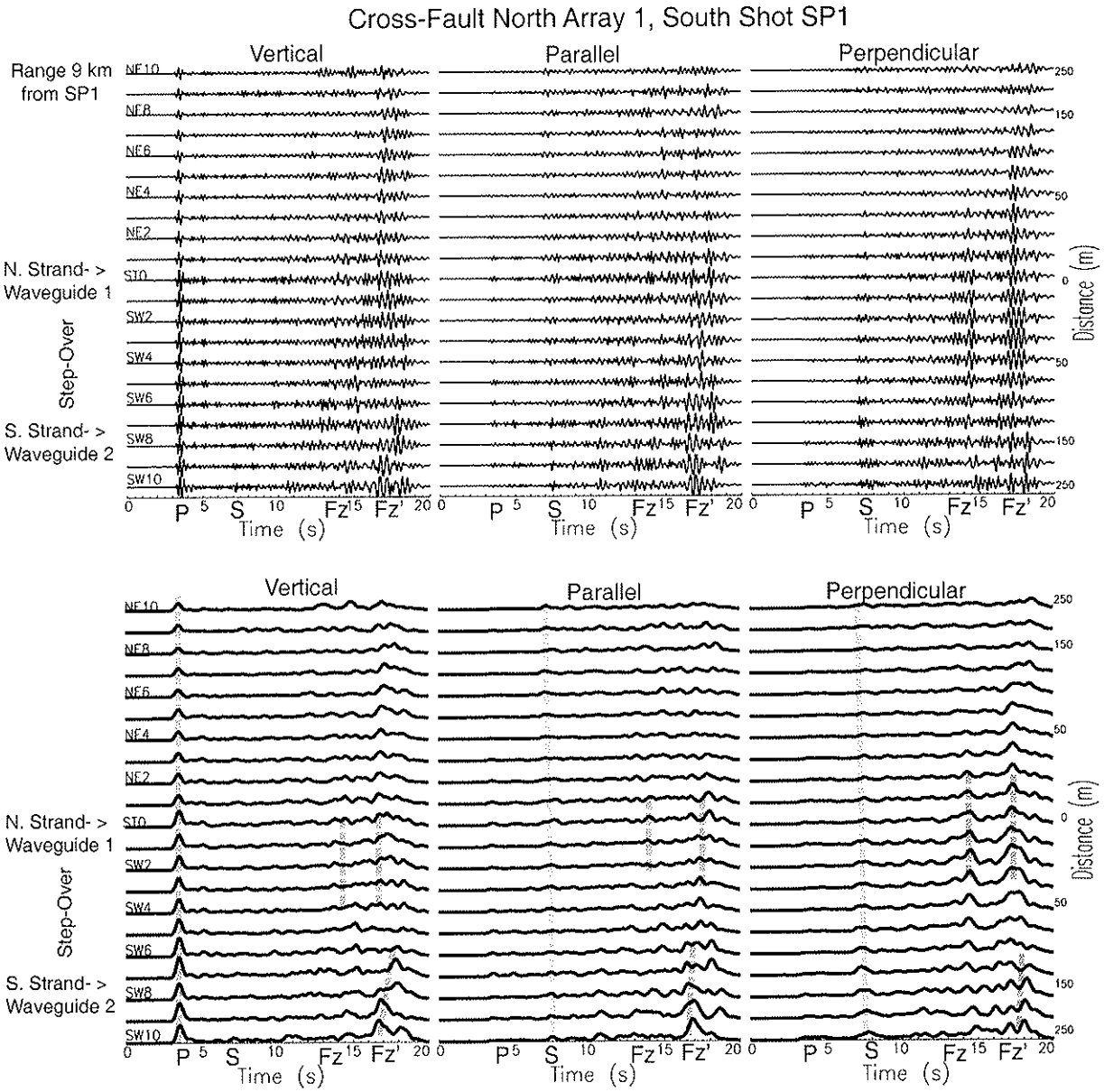

Figure 3b. top: Three-component seismograms recorded at the north Array 1 across the SHF in the step-over for the south shot SP1 detonated within the southeast rupture segment at the distance (range) of 9 km southeast of the array. Seismograms have been band-pass (2-7 Hz) filtered and are plotted using a common scale for all traces. P and S waves arrive at ~3.5 s and ~7 s. Fault-zone trapped waves with large amplitudes and long duration between 12 s and 18 s at stations on the southwest part of the array. Fz and Fz denote the early and late trapped waves. Note that traveltimes of P, S and trapped waves from SP1 and SP2 t of Array 1 are not linearly proportional to the distance between the two shots and the array, indicating the velocities increase with depth because the waves from the farther shot SP1 penetrate the deeper crust. bottom: Envelopes of waveforms are plotted using a common scale for all traces, showing large amplitudes of trapped waves at stations on the southwest part of the array that were located in the fractured damage zone in the step-over between the north and south rupture segments. The red, green, and blue dashed lines align with the peaks of P, S, and trapped waves, respectively. Note that amplitude peaks of trapped waves indicate two low-velocity waveguides on the northwest and southeast rupture segments, respectively. Since shot SP1 was located on the southeast rupture segment but the center of Array 2 was located on the northwest rupture segment, we interpret that the two rupture segments may connect together at depth beneath the surface step-over. The width of the waveguides inferred by trapped waves is ~75 m. Other notations are the same as in Fig. 3a.

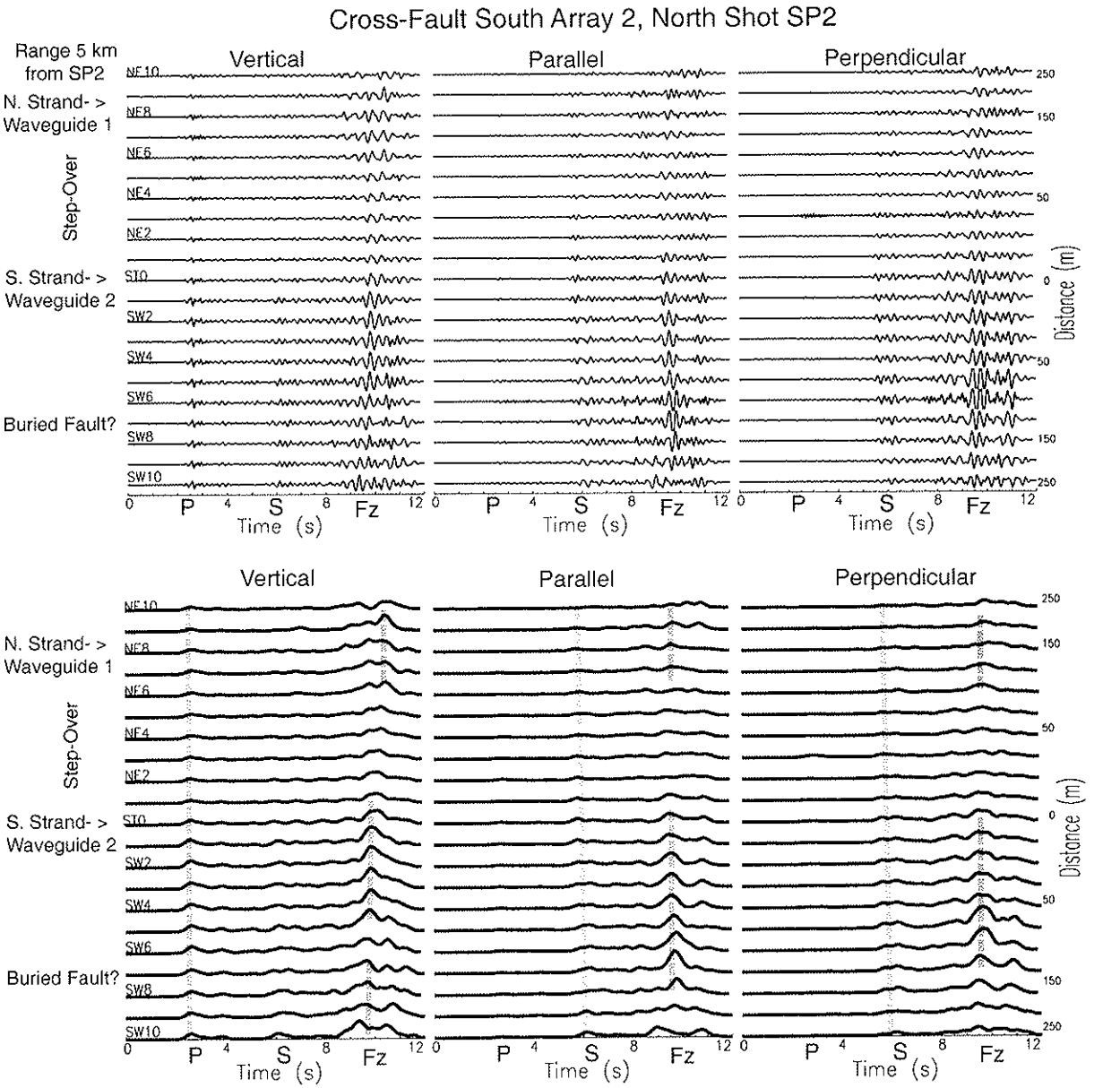

Figure 4a. top: Three-component seismograms recorded at the south Array 2 across the SHF in the step-over for the north shot SP2 detonated within the northwest rupture segment at the distance (range) of 5 km northwest of the array. Station ST0 of the array was located on the southeast fault strand while the northeast part of the array intersected the extension of the northwest fault strand in the step-over. Seismograms have been band-pass (2-7 Hz) filtered and are plotted using a common scale for all traces. P and S waves arrive at ~2.7 s and ~5.8 s. Fault-zone trapped waves with large amplitudes and long duration between 9 s and 11 s at stations on the southwest part of the array. However, note that trapped waves were also registered at stations located close to t he northwest fault strand in the step-over. Since shot SP2 was located on the northwestrupture segment but the center of Array 2 was located on the southeast rupture segment, again showing that the two rupture segments may connect together beneath the surface step-over. bottom: Envelopes of waveforms are plotted using a common scale for all traces, showing large amplitudes of trapped waves at stations in a distance range of 150 m southwest to the southeast fault strand, suggesting that the low-velocity waveguide lies on the southwest side of this fault strand, consistent with the greater postseismic displacement observations across the southeast rupture segment (Fig. 2a). Other notations are the same as in Fig. 3a.

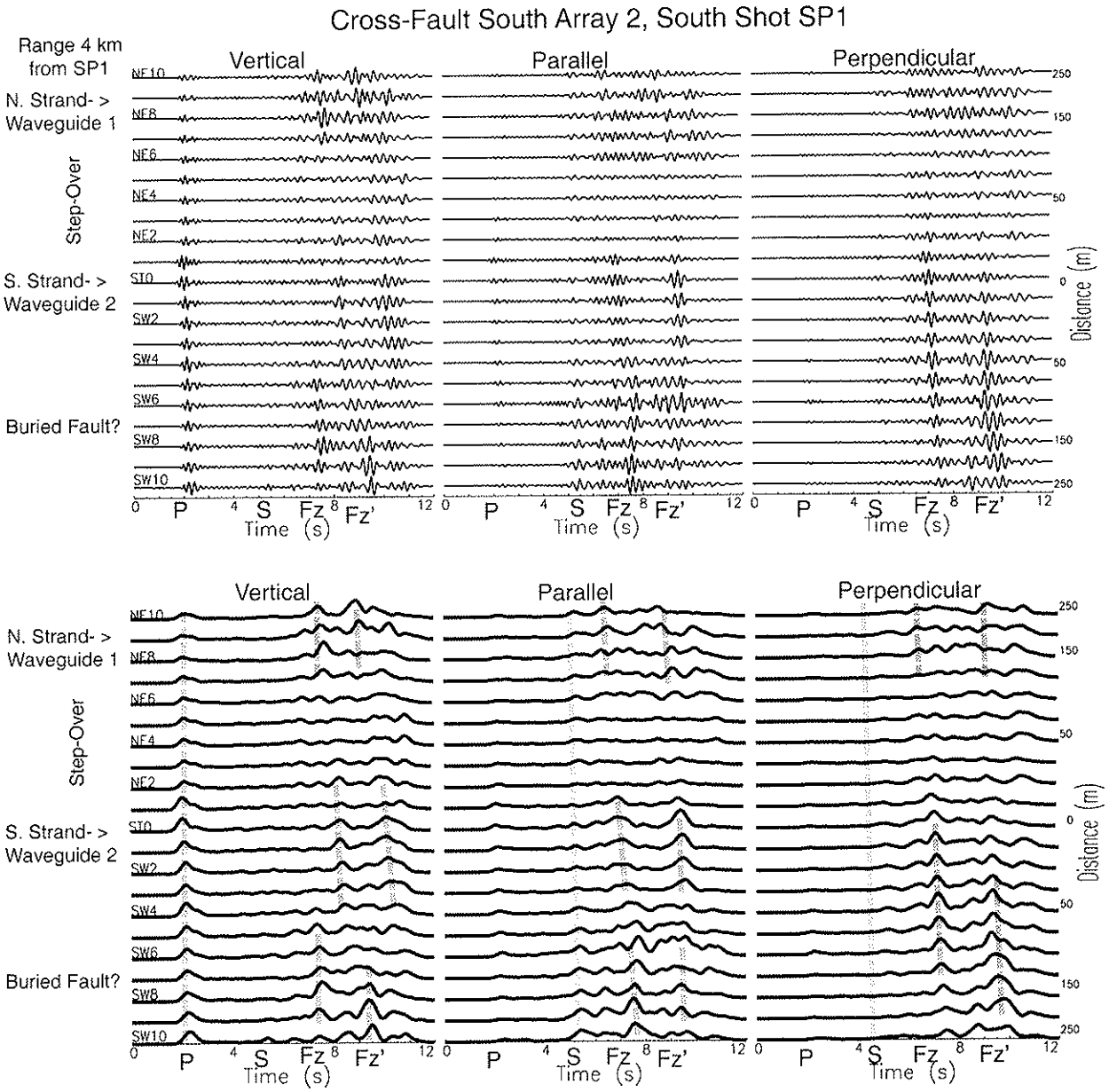

Figure 4b. top: Three-component seismograms recorded at the south Array 2 across the SHF in the step-over for the south shot SP1 detonated within the southeast rupture segment at the distance (range) of 4 km southeast of the array. Seismograms have been band-pass (2-7 Hz) filtered and are plotted using a common scale for all traces. P and S waves arrive at ~2.2 s and ~5 s. Fault-zone trapped waves with large amplitudes and long duration between 7 s and 10 s at stations on the southwest part of the array. However, note that trapped waves were also registered at stations located close to the northwest fault strand in the step-over, again indicating that the southeast and northwest rupture segments connect at depth beneath the surface step-over. bottom: Envelopes of waveforms are plotted using a common scale for all traces, showing large amplitudes of trapped waves. Note that amplitude peaks of trapped waves appeared at stations close to the southwest fault strand but also at stations SW6-10 of Array 2. We speculate that there is a buried fault lying southwest of the southeast rupture segment and it also ruptured in the 1987 mainshock but did not expose to the surface, Other notations are the same as in Fig. 4a.

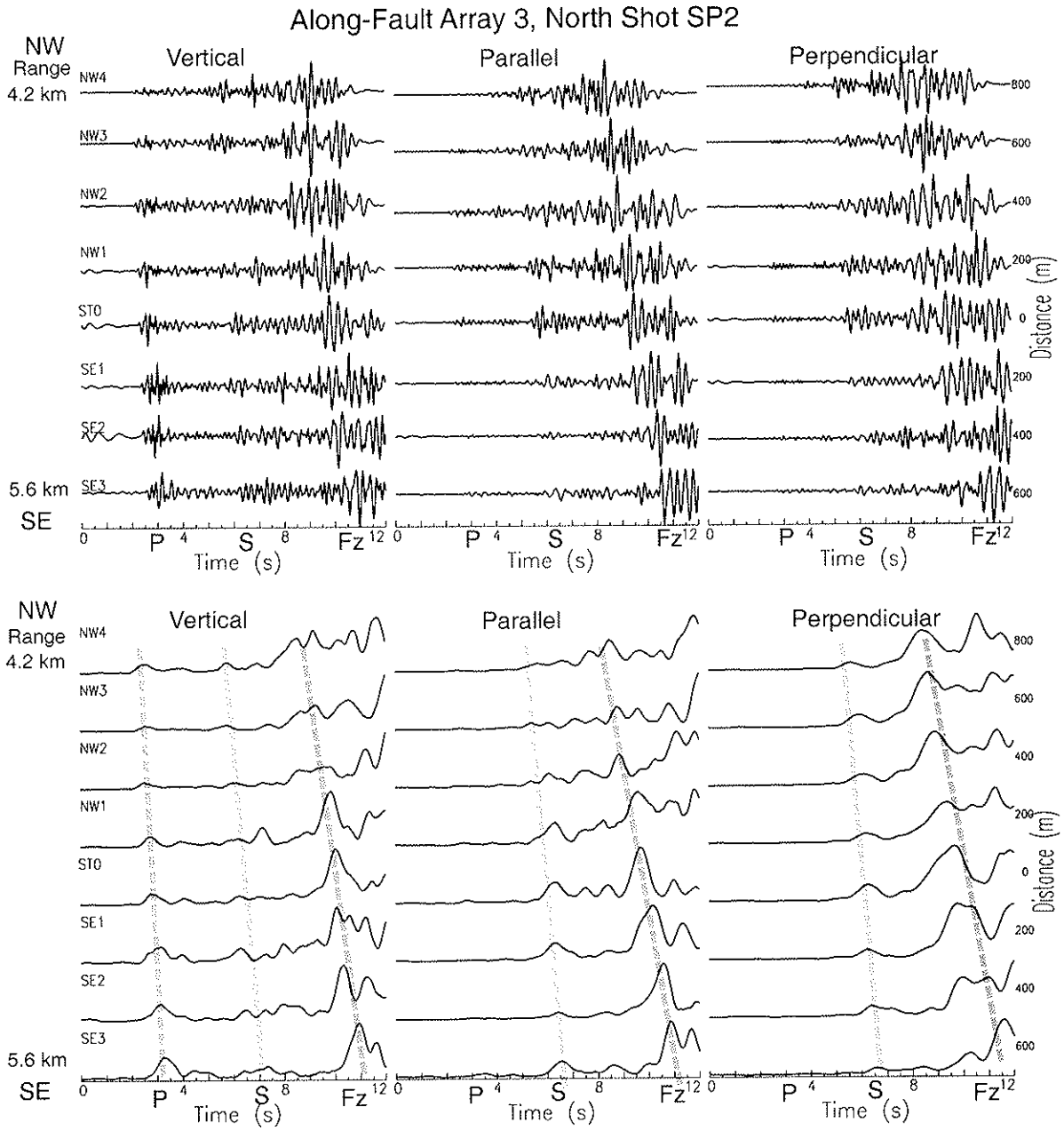

Figure 5a. top: Three-component seismograms recorded at the 1.4-km-long Array 3 along the SHF for the north shot SP2 detonated within the northwest rupture segment at the distance (range) of 4.2 km northwest of the array. Station ST0 of the along-fault array was co-located at the center of the south cross-fault Array 2. Seismograms have been band-pass (2-7 Hz) filtered and are plotted in trace-normalized. bottom: Envelopes of waveforms are plotted in trace-normalized. The red, green, and blue dashed lines align with the peak amplitudes of P, S, and trapped waves, respectively. The separation between the S and fault-zone trapped waves increases with the distance, showing the existence of a continuous low-velocity waveguide along the SHF, and also showing the connection of the northern rupture segment to the southern rupture segment at depth. Based on the slopes of dashed lines, velocities of P, S , and trapped waves are measured to be ~2 km/s, 1.0 km/s, and 0.7 km/s, respectively at the shallow depth.

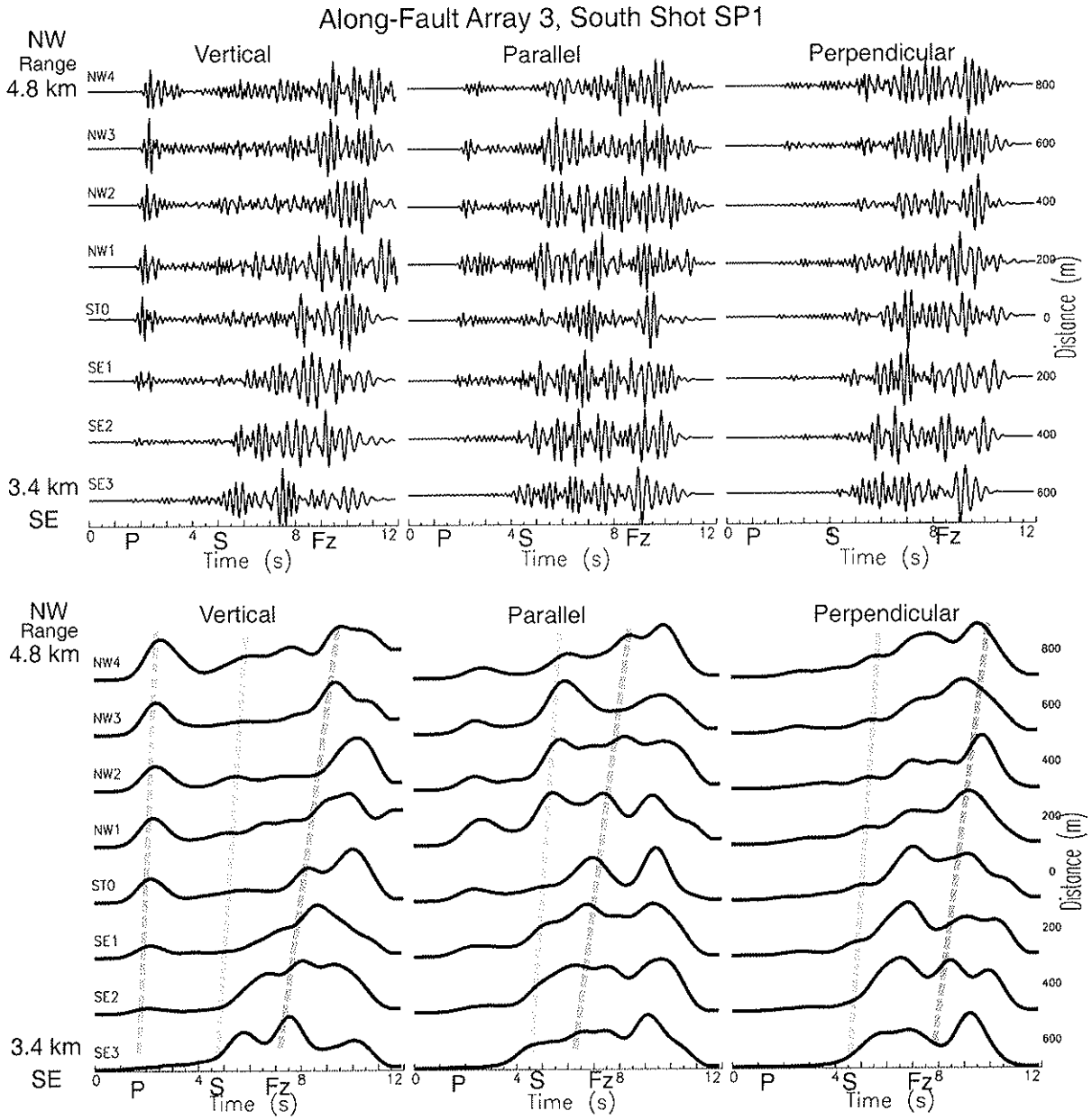

Figure 5b. top: Three-component seismograms recorded at the 1.4-km-long Array 3 along the SHF for the south shot SP1 detonated within the northwest rupture segment at the distance (range) of 3.4 km southeast of the array. Seismograms have been band-pass (2-7 Hz) filtered and are plotted in trace-normalized. bottom: Envelopes of waveforms are plotted in trace-normalized. The red, green, and blue dashed lines align with the peak amplitudes of P, S, and trapped waves, respectively. The separation between the S and fault-zone trapped waves increases with the distance, showing the existence of a continuous low-velocity waveguide along the SHF, and also showing the connection of the northern rupture segment to the southern rupture segment at depth. Based on the slopes of dashed lines, velocities of P, S , and trapped waves are measured to be ~2 km/s, 1.1 km/s, and 0.8 km/s, respectively at the shallow depth. Other notations are the same as in Fig. 5a.

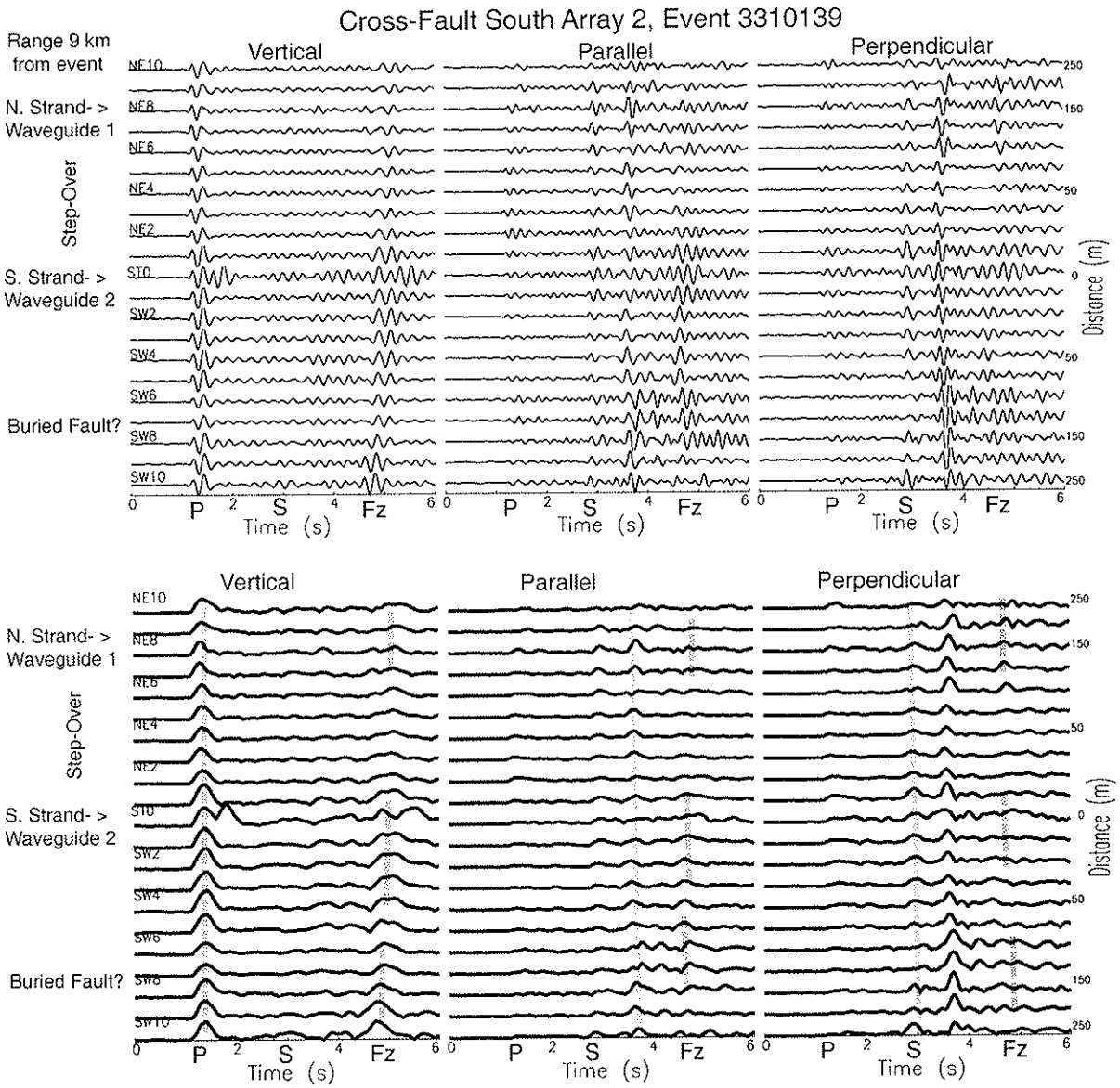

Figure 6a. top: Three-component seismograms recorded at the south Array 2 across the SHF in the step-over for a microearthquake (November 24, 2000) occurring on the SHF at the depth of ~8 km and ~3 km northwest of the array. Seismograms have been band-pass (2-7 Hz) filtered and are plotted using a common scale for all traces. Fault-zone trapped waves with large amplitudes and long duration following S waves appeared at stations on the southwest part of the array. However, trapped waves were also registered at stations located close to the northwest fault strand in the step-over, again indicating that the southeast and northwest rupture segments connect at depth beneath the surface step-over. bottom: Envelopes of waveforms are plotted using a common scale for all traces, showing large amplitudes of trapped waves. Note that amplitude peaks of trapped waves appeared at stations close to the southwest fault strand but also at stations SW6-10 of Array 2, again indicating that there is a buried fault lying southwest of the southeast rupture segment and it might rupture in the 1987 mainshock but did not expose to the surface, Other notations are the same as in Fig. 4a.

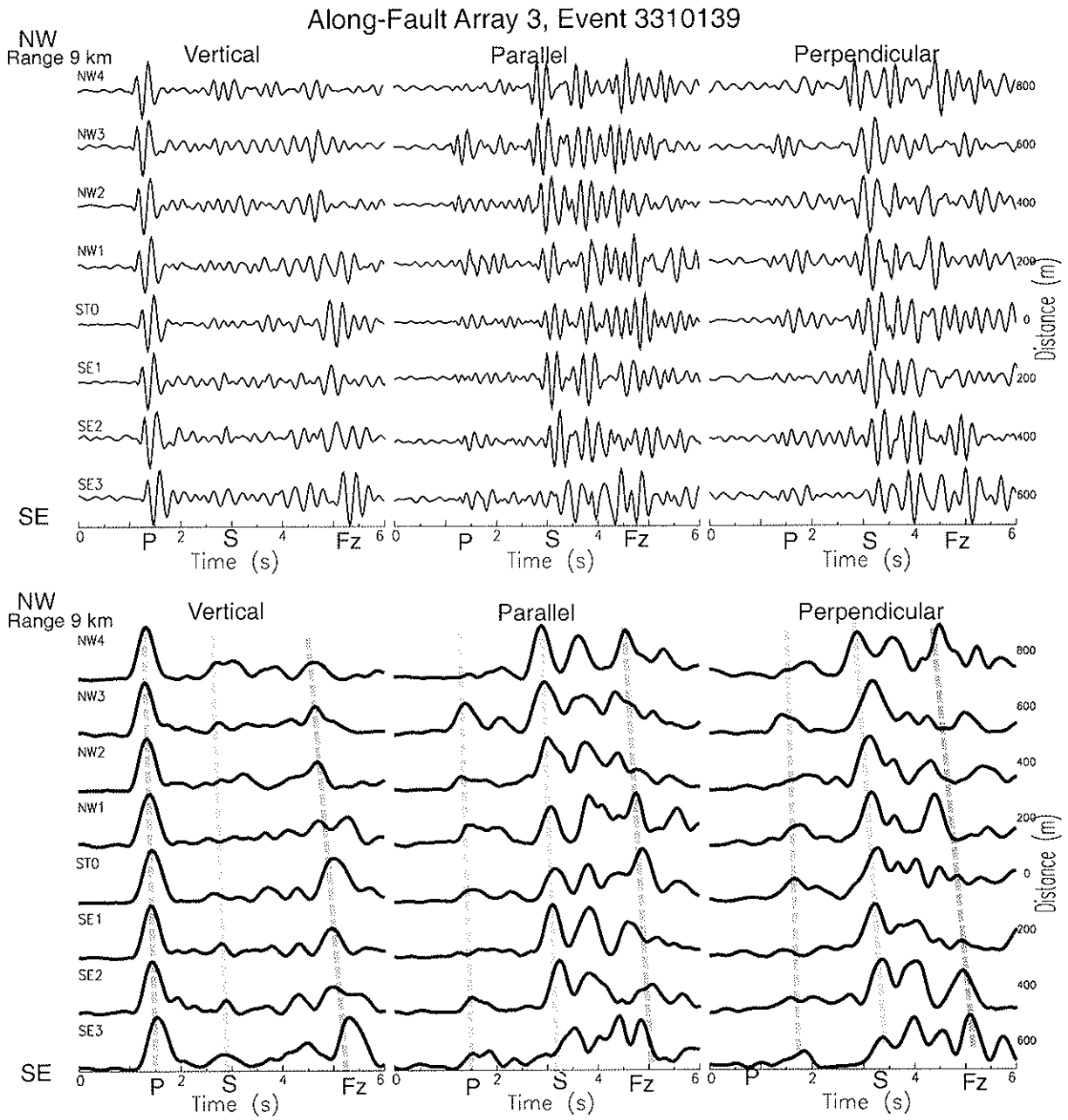

Figure 6b. top: Three-component seismograms recorded at the 1.4-km-long Array 3 along the SHF for a microearthquake (November 24, 2000) occurring on the SHF at the depth of ~8 km and ~3 km northwest of the array. Seismograms have been band-pass (2-7 Hz) filtered and are plotted in trace-normalized. bottom: Envelopes of waveforms are plotted in trace-normalized. The separation between the S and fault-zone trapped waves increases with the distance, showing the existence of a continuous low-velocity waveguide along the SHF, and also showing the connection of the northern rupture segment to the southern rupture segment at depth. Other notations are the same as in Fig. 6a.

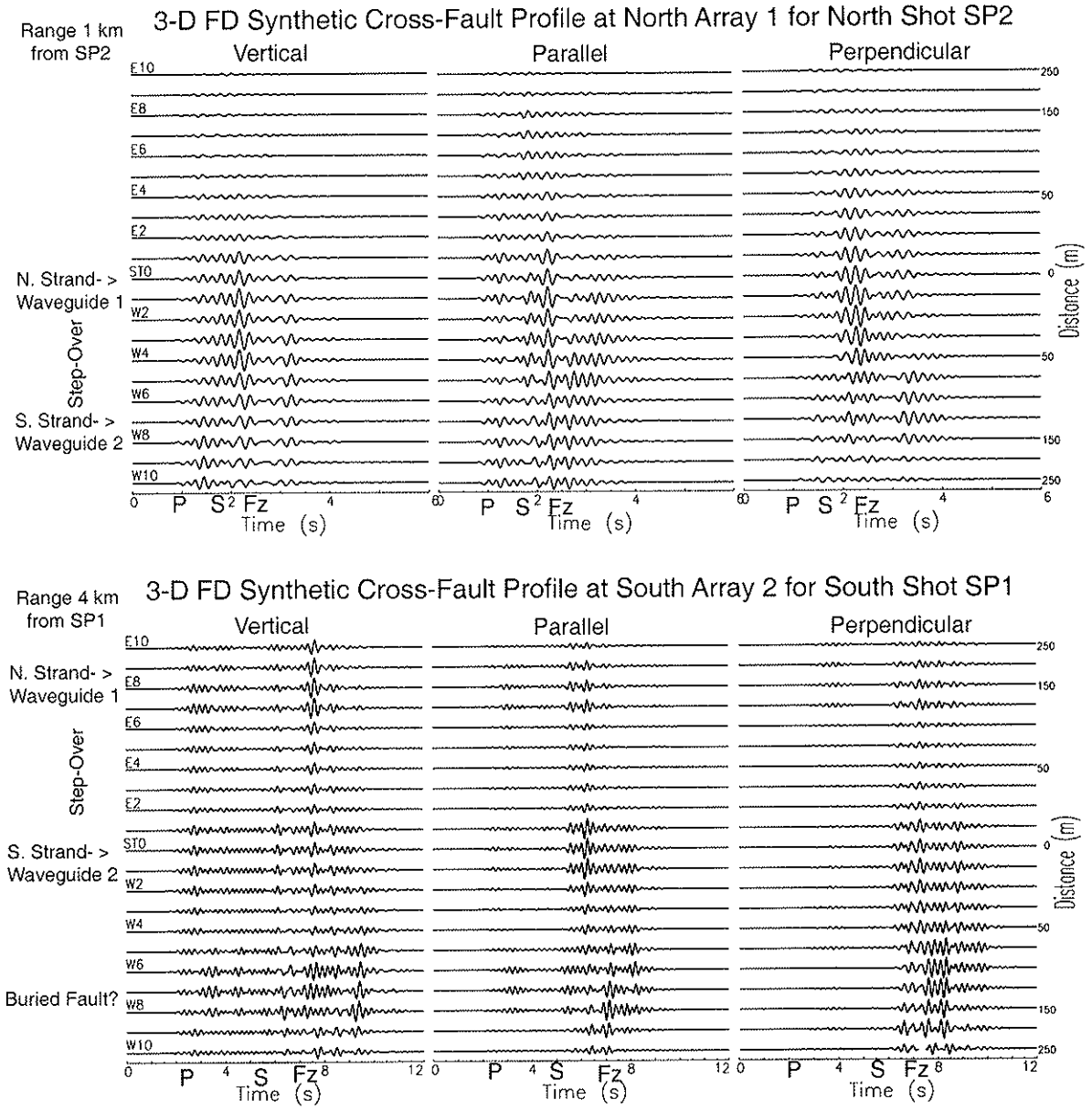

Figure 7. Examples of three-component synthetic seismograms using 3-D finite-difference code (top) for north Array 1 across the SHF and north shot 2, and (bottom) for south Array 2 and south shot SP1. Model parameters are given in Figure 8b. The 75-m-wide low-velocity waveguides on the northwest and southeast rupture segments of the Superstition Hills fault connect at the depth of 1 km. The waveguide on the blind fault connects to the SHF at depth too. An explosion source is applied within the northwest waveguide at the distance of 1 km from Array 1 in the first example while is applied within the southeast waveguide at the distance of 4 km from Array 2 in the second example. The synthetic seismograms are comparable with observations (Figures 3a and 4b) in the zero-order sense. The best-fit model parameters will be resulted from a more systematic simulation of fault-zone trapped waves generated by explosions and microearthquake as well Other notations are the same as in Fig. 3a and Fig.4b.

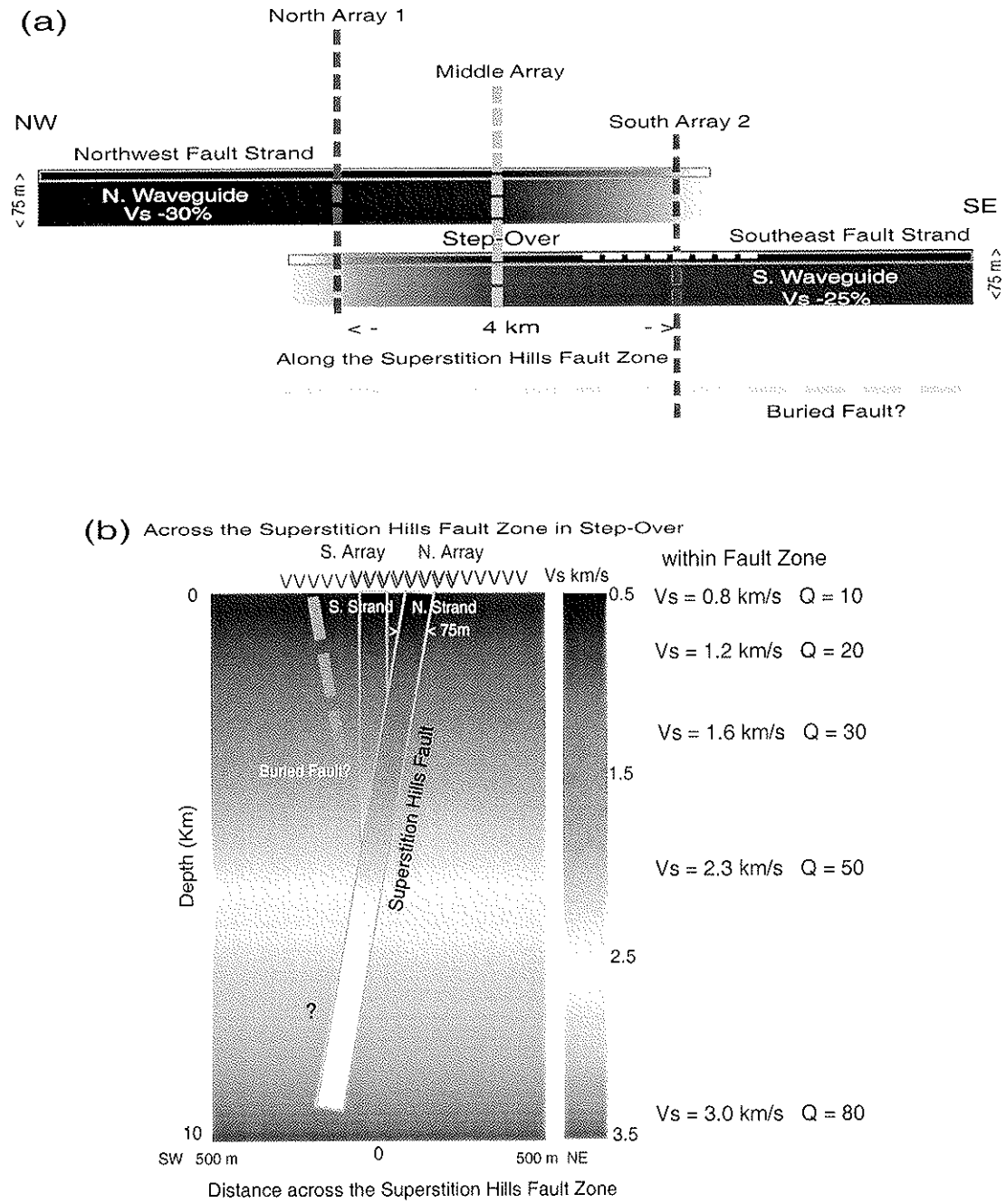

Figure 8. (a) Map view along the Superstition Hills fault zone at the 4-km-long step-over. Blue bars denote low-velocity waveguides along the northwest and southeast rupture segments of the 1987 M6.6 earthquake. The waveguide is ~75 m wide. Black lines in the waveguide denote The northwest and southeast fault strands are marked by black lines in in the waveguides. The dark color denotes new breaks while light color denotes extension of the strand. Three linear seismic arrays (N. Array 1, S. Array 2, and Middle array) across the NW and SE fault strands in the step-over are marked by the blue, red, and green dashed lines. The along-fault array is marked by the dashed yellow line. The grey dashed line denotes a buried fault southwest of the southeast rupture zone. It may be the northwest extension of the Wiener fault which ruptured and exposed to the surface in the 1987 earthquake. (b) The depth section across the Superstition Hills fault zone at the step-over. The north seismic Array 1 and south Array 2 are across the 1987 northwest and southeast rupture segments. The fault-zone trapped wave inferred low-velocity waveguides along the northwest and southeast fault strands are ~75 wide, within which the velocities are reduced by 25-30% from wall rock velocities and Q values are 10-80 at depth from 0 to 10 km. Two waveguides may connect at depth and may dip to southwest, according to the locations of aftershocks of the 1987 M6.6 earthquake (Fig. 1). The waveguide velocities and Q given in the figure are used to synthesize fault-zone trapped waves shown in Figure 7. The vertical grey dashed line denotes a buried fault which is probably the northwest extension of the Wiener fault.